25th ABCM International Congress of Mechanical Engineering
October 20-25, 2019, Uberlândia, MG, Brazil

# COB-2019-0001
# EFFECT EVALUATION OF THE ADHESIVE THICKNESS VARIATION IN SINGLE LAP JOINTS BONDED WITH STRUCTURAL ADHESIVE

## XXV COBEM

**Lorena Pessanha Silva**
Federal University of Rio de Janeiro, Aloísio da Silva Gomes Ave, 50, 27930-560, Macaé, RJ, Brazil. E-mail: Lo.pessanha@outlook.com
**Ranulfo Martins Carneiro Neto**
Federal University of Rio de Janeiro, Aloísio da Silva Gomes Ave, 50, 27930-560, Macaé, RJ, Brazil. E-mail: ranulfocarneiro@yahoo.com.br
**Eduardo Martins Sampaio**
Rio de Janeiro State University, Laboratory of Adhesion and Adherence, Bonfim St, 25, 28625-570, Nova Friburgo, RJ, Brazil. E-mail: edu.msampaio@gmail.com
**Lucas Lisbôa Vignoli**
Federal University of Rio de Janeiro, Aloísio da Silva Gomes Ave, 50, 27930-560, Macaé, RJ, Brazil. E-mail: lucaslvig@gmail.com

***Abstract.*** *The use of bonded joints is increasing as an alternative way of mechanical joining such as weld, bolt and nut or rivets. This occurs, besides other aspects, because the weight reduce, facility of joining both different or same materials and more uniform stress distribution along the adhesive. To design bonded joints with more reliability, it is essential to understand stresses states between the material and the adhesive. This paper presents experimental results of single lap joints (SLJ) in accordance with ASTM 1002 standard. The specimens were bonded with a structural adhesive for three different thickness: 0,4mm, 0,8mm and 1,5mm. The joints of each group were modelled numerically using the cohesive zone model (CZM), being these results compared with the experimental values. The aim is to verify if the CZM also works well for large thicknesses. In order to obtain the critical energy release in mode I and II ($G_{Ic}$ and $G_{IIc}$, respectively) the Taperad Double Cantilever Beam (TDCB) and End Notched Flexure (ENF) tests were performed. The comparison between both numerical and experimental simulations were satisfying only to the adhesive thickness of 0,4mm and 0,8mm.*

**Keywords:** *Bonded joints, adhesive thickness, cohesive zone model, single lap joint.*

## 1. INTRODUCTION

The utilization of adhesive bonding technology is increasing in several areas, especially in the automotive and aeronautic industry as well as oil and gas and construction industry. This technology has some advantages when compared with traditional methods of joining such as fastening, riveting or welding. The benefits include: better uniform distribution of stresses along the bonding region since fastening expose the material to concentrated stresses, the capability of joining different material since the adhesive provides corrosion prevent, reduction in weight since the adhesive has lower density than steel (Barnes and Pashby, 1998).

The study of bonded joint aims to evaluate the bonded line, which provides the joining between adherents (Ribeiro, 2009). This is not so simple, because bonded joints have a complex behavior mechanical, followed by the difficulties in preventing it (Da Silva, 2010). Besides it's great advantages, the use of bonded joints is restricted due to the several different factors that influences the joint. According to Kim et al. (2008) the failure loads are not linearly proportional to the bonding length. The author affirm that the edges of the bonded line play a more important role in the load transfer.

The determination of the bonded joints behavior is still a limitation of this technology (da Silva, 2010) because many aspects influences the joint strength. Several studies have been made trying to understand these influences. Among, they include joint geometry - studied by (Kafkalidis, 2002), (Lang, 1998), surface treatment – studied by (Shahid, 2002), (da Silva *et al.*, 2009b), and thermal effects – studied by (Adams *et al.,*1992) and (Apalak and Gunes, 2002). The focus of this work is to study the variation of the joint geometry, specifically the adhesive thickness influence in the joint strength.

According to da Silva *et al.* (2007), in single lap joints a large percentage of the strength is concentrated in the joint ends. Therefore, changes in the geometry of substrate leads into relief of those tensions (Neto, 2019). Another study

treating the same subject was done by Pandey (1999) apud da Silva (2010), which indicates that an increase of substrate thickness reduces shear stress concentration. Therefore, thicker plates tend to keep the tension distribution more uniform.

According to Gleich *et al.* (2001) *apud* Nascimento (2013), it is necessary to guarantee an optimum thickness of adhesive (between 0,1mm and 0,5mm). On mostly bonded joints applications, the suppliers recommend a thickness between 0,1 mm and 0,2 mm to get the maximum resistance.

Crocombe (1989) apud Neto (2017) shows in his study that thicker joints present failure first when submitted to shear stresses. Adams and Peppiatt (1974) assigned the effect of decreasing the resistance with the increase of adhesive thickness due to the fact of existence of internal flaws on adhesive, as a consequence of healing process. Naito et al (2012) apud Nascimento (2013) measured the influence of adhesive thickness on single lap joint exposed to shear and peeling stresses. The thickness varies according to: 0,1, 0,3, 0,5 and 1 mm with adhesives made by polyamide. As a result, for the 1,0 mm thickness the joint strength was lower than with the thinner thicknesses. Da Silva (2010) analyzed the joint L strength exposed to pure shear stress and combined loading (shear and tension), considering in both cases the variation of the bonded area. The conclusion is that the height (h) plays a more important role than width (w) if compared to the tensile strength.

Currently, there are two mathematical approaches to predict a bonded joint behavior: using the analytical method and the numerical method (Neto, 2017). Both use differential equations to predict the joint performance. The simpler analytical models considered only the elastic behavior of materials and only deformations derived from shear stresses. Volkersen and Goland and Reissner were the pioneers in the development of analytical models (Carvalho, 2016). Volkersen considered that the adhesive and adherent have a elastic behavior. They assumed that the adhesive strains only in shear, but the adherends can strain in tension (da Silva *et al.*,2009b).

The shear stress has maximum values at overlap ends, and it is considerably lower in the middle, as shown in Fig. 1. However, this classical model does not consider the bending effect caused by the load eccentricity (Neto, 2017). Furthermore, the model considers that the maximum stress occurs at the end, which violates the stress-free condition. This topic was considered by Renton and Vinson (1975). They showed that the shear stress state at the adhesive ends has a null value.

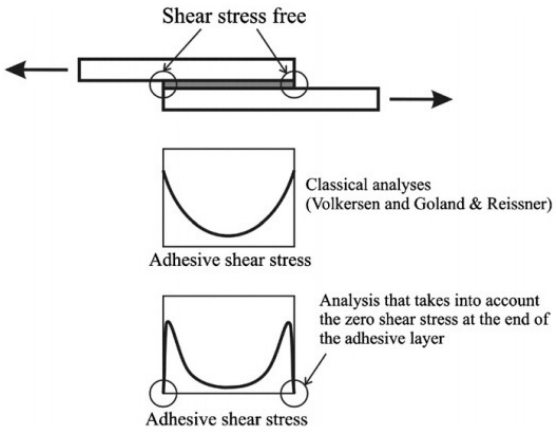


Figure 1. Adhesive shear stress distribution when the stress free condition at overlap ends occurs (Da Silva, 2007).

Even though the analytical studies performed being very important in the stress analysis of adhesively bonded joints, the analytical models have several limitations. In order to complement the analytical models, the numerical models emerged. The most used one is the Finite Elements Method (FEM), which is usually used to study the behavior of a bonded joint and can be used to validate analytical models. For single lap joints (SLJ) the simulation must provide the failure load and should describe the tensions especially in overlap length. Some software have already incorporated in their system the cohesive zone model (CZM) which is used to predict the bonded behavior.

According to Medina (2014) and Fiuza (2016), the traditional concepts of mechanical of materials do not consider the fracture toughness, which can be defined as a property that quantify the resistance against crack propagation. Therefore, the linear elastic fracture mechanics (LEFM) investigate the materials performance with discontinuities. As stated by Fiuza (2016), the LEFM considerer two basic requirements: the one that uses a stress intensity factor and the other one is based on energy concepts.

According to Neto (2017) the energy criterion uses strain energy release rate ($G_I$ and $G_{II}$) and the critical strain energy release rate in shear and traction known as $G_{Ic}$ and $G_{IIc}$. In order to obtain these properties, the three main modes of loads indicated in figure 2 should be understood:

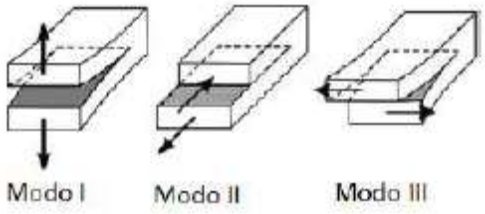


Figure 2. Main configuration of loads (Carvalho, 2016).

As shown in Fig. 2 the mode I considers only tractions stresses, while mode II and III only contemplate shear stresses (Neto, 2017). For mode I the DCB and TDCB are the most commonly used tests. Through these tests, the value of $G_{Ic}$ can be obtained. Bautista (2008) claims that although in practices occurs the combination of the three modes, the mode I is the most important, because in many cases this is the prevailing load and it is the simpler to be analyzed. For mode II the most used test to calculate $G_{IIc}$ and $G_{IIIc}$ is the End Notched Flexure (ENF). Despite there is no standard to define this test, there are several articles in the literature with good results (Neto, 2017).

The numerical simulation can be performed using the Cohesive Zone Model (CZM), which use the concepts of linear elastic fracture mechanics (LEFM). This model has the capacity of predicting the behavior of damage and its evolution (Neto, 2017). It occurs because artificially cohesive elements are introduced in the adjacent pairs, where the damage propagation is caused by the existence of a discontinuity (Carvalho, 2016). This configuration is ruled by the traction separation-law, that considerer firstly an elastic behavior forwarded by the onset and propagation of damage on material. There are three main configurations of the traction-separation law: triangular, exponential and trapezoidal. The choice of which one will be used depends on the material behavior and the interface between substrate and adhesive.

The triangular model, used in this paper, is graphically represented by the relation between the tensions and relative displacements between the pairs of cohesive elements (Fig. 3).

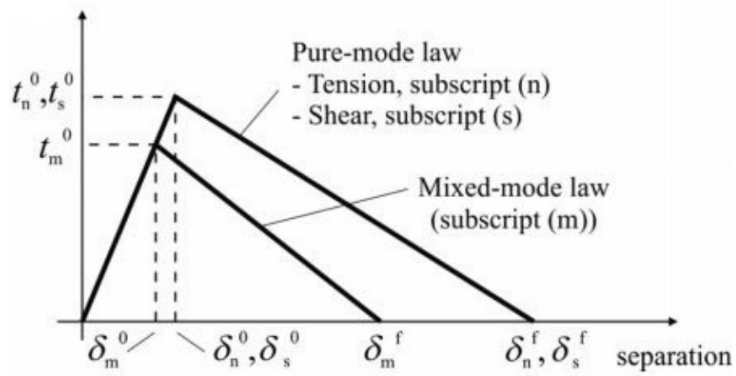


Figure 3: Cohesive Zone Model in triangular configuration (Neto, 2017).

The subscript "$n$" and "s" represent the configuration with pure traction and pure shear, respectively. If a mixed mode occurs, the subscript "$m$" is used. The material remains elastic until it reaches the traction pure modes ($t_n^o$ e $t_s^o$), in case of pure mode, and $t_m^o$ in case of mixed mode. By this time, the displacements are $\delta_n^0$ and $\delta_s^0$ (pure mode) or $\delta_m^0$(mixed mode), and so the material starts to lose its stiffness and then the damage propagates until it completes total failure. The $G_{Ic}$ and $G_{IIc}$ represents the area of this traction-separation graphic. The definition of the maximum displacements ($\delta_n^f$ and $\delta_s^f$, for pure mode and $\delta_m^f$ for mixed mode) is performed by making $G_I = G_{IC}$ and $G_{II} = G_{IIC}$.

For this model a criterion must be established in order to determine the onset and evolution of the damage. The variables $t_n^o$, $t_s^o$, $t_t^o$ refers to the peak of traction-separation graphic, being the subscript "$n$" representing the traction pure mode, and "*s*" and "*t*" representing the shear pure mode. In this paper the parameter used to characterize the initiation of the damage was quadratic stress criterion. In this criterion the damage onset occurs when the equality of the Eq. 4 is satisfied.

$$\left\{\frac{\langle t_n \rangle}{t_n^o}\right\}^2 + \left\{\frac{t_s}{t_s^o}\right\}^2 + \left\{\frac{t_t}{t_t^o}\right\}^2 = 1 \tag{1}$$

The damage evolution selected to this article is based on energetic criteria which is implemented by the software inputting the fracture energy ($G_c$). Since we choose the criterion, the program guarantees that the area below the graphic curve is the fracture energy (Abaqus, 2014).

The fracture criterion used as input to the software was the power law fracture criterion. This method considers that the fracture is ruled by the energy needed to cause fracture in the material, according to Equation 5:

$$\left\{\frac{G_I}{G_{Ic}}\right\}^{\alpha} + \left\{\frac{G_{II}}{G_{IIc}}\right\}^{\alpha} + \left\{\frac{G_{III}}{G_{IIIc}}\right\}^{\alpha} = 1 \quad (2)$$

The most common values for α is 1, when the linear criteria is used, and 2, when the quadratic criteria is used. The inputs required are the fracture energy in traction mode ($G_{Ic}$) and shear mode ($G_{IIc}$ and $G_{IIIc}$). The properties of substrates and adhesives, such as Young 's modulus, Poisson's ratio, maximum stresses (normal and shear), are also required.

The aim of this work is to verify if the CZM works well to larger thickness, specially 0,8 mm and 1,5 mm. In a recent work, Neto (2017) studied combined loading joint (L joint) with two points of force application (50 mm and 100 mm from the adhesive layer. Two adhesive thickness was studied: 0,4 mm and 1,5 mm. The comparison between experimental and numerical results were satisfied only to 0,4 mm. Thus, this work aims to investigate if the same occurs to single lap joints. One more adhesive thickness was added to check if with 0,8 mm thickness (mean value) the CZM leads to accurate results. The simulation was performed inn Abaqus, using 2D models.

## 2. MATERIALS AND METHODS

The basic arrangement for a single lap joint test is shown on Fig. 4. The force (F) is applied by a tensile machine. The overlap length is represented by the letter *L*, *w* is the width and $t_p$ e $t_a$ are the thickness of both substrate and adhesive, respectively.

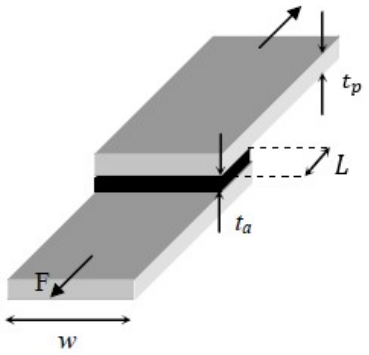


Figure 4. Single lap joint configuration (Da Silva, 2010).

For the experimental test the specimens were manufactured with two metal sheets made by A36 and bonded with adhesive ARC 858. The properties of ARC 858 were obtained according to standard ASTM D 638-03 dimensions. A total of thirty specimens were bonded with ARC 858, with three different adhesive thickness: 0,4, 0,8, 1,5 mm, ten specimens for each thickness. They were tested in a single lap joint configuration according to standard ASTM 1002. The specimens were tested using an Autograph Precision Universal Testing Machine Shimadzu model AG-X Plus 100 KN (Figure 5). Two sheets of metal A36 with the thickness recommended by standard ASTM 1002 were placed between the machine clamps (Fig. 5), taking special care that the bending moment does not interfere in final results.

In order to determine the $G_{Ic}$ and $G_{IIc}$ the TDCB and ENF tests were performed for 0,8 mm thickness. To the 0,4 mm and 1,5 mm adhesive thickness, the properties were obtained from the work of Neto (2017). It includes the Young's module ($E$), shear module (G*)*, Poisson's ratio (ν), maximum normal stress ($t_n$) and maximum shear stress ($t_s$).


Figure 5. Schema used to test the specimens.

## 3. RESULTS

The adhesive properties listed in Table 1 (mechanical properties) were obtained from the work of Neto (2017). The data from Table 2 (cohesive properties) were obtained from the same cited work (Neto, 2017) for the thickness 0,4 and 1,5 mm. The values for the 0,8 mm thickness were obtained by the TDCB and ENF tests, performed at this work. These properties are inputs to the Abaqus bonded joints simulation.

Table 1. Adhesive properties regarding all thicknesses.

| **Mechanical Properties** | |
|---|---|
| Young's modulus - $E$ | 7073,03 ± 64,02 MPa |
| Shear modulus - $G$ | 2660,82 MPa |
| Poisson's ratio - ν | 0,33 ± 0,01 |
| Tensile failure strenght - $t_n^o$ | 28,96 ± 1,10 MPa |
| Shear failure strenght - $t_s^o$ | 18 MPa |

Table 2. $G_{Ic}$ and $G_{IIc}$ for the three different thickness.

| **Cohesive Properties** | | ***Thickness (mm)*** | | |
|---|---|---|---|---|
| | | **0,4** | **0,8** | **1,5** |
| Fracture energy in tension - | $G_{Ic}$ | 0,135 ± 0,05 N/mm | 0,353 ± 0,03 N/mm | 0,21 ± 0,06 N/mm |
| Fracture energy in shear - | $G_{IIc}$ | 2,025 ± 0,351 N/mm | 3,23 ± 0,25 N/m | 1,30 ± 0,264 N/mm |

The bonded joint was drawn on Abaqus with the same test dimensions. For the substrates, four-node solids elements with reduced integration (CPE4R) were used, which are two-dimensional quadrilateral elements with plane deformation state. Cohesive elements (COH2D4 from Abaqus), also with 4 nodes, were used for the adhesive layer. Two boundary conditions were settled: one end was embedded and the other end a horizontal displacement was applied. Besides that, the energy concept was used in this article.

Several converging problems appeared at the simulation. So, the steps were changed in order to guarantee that all three adhesive thickness simulations converged, also the displacement value was edited. As occurred in the work of Neto (2019), a mesh density did not influence the rupture force, considering the type of loading and boundary conditions presented. The results are shown in Fig. 6.

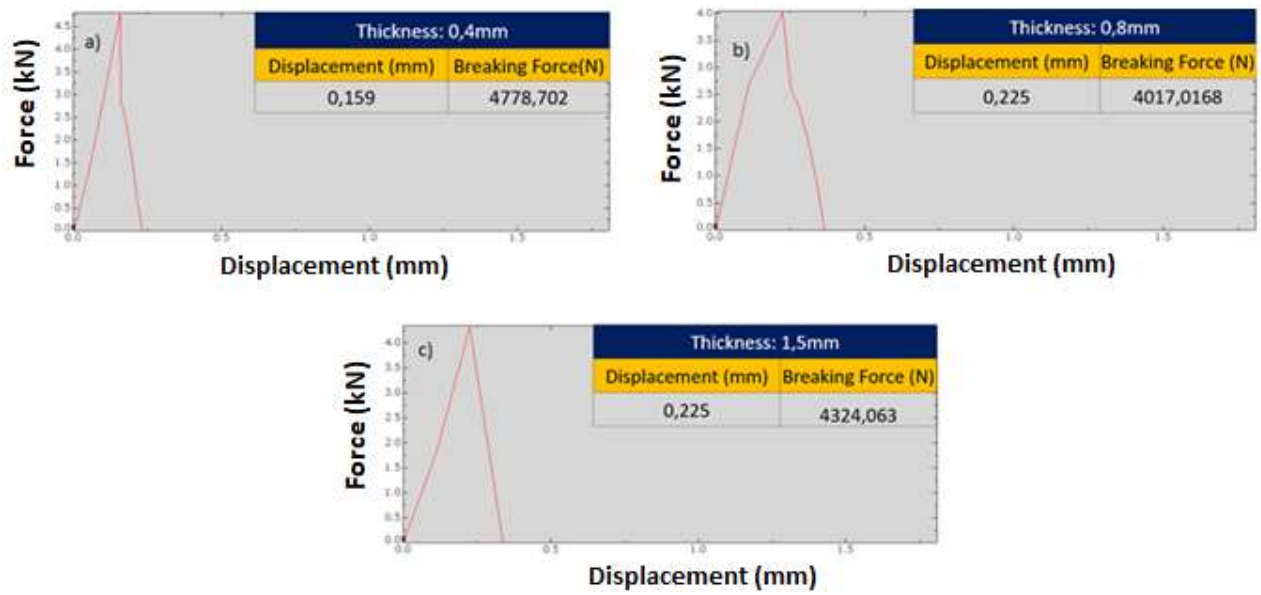


Figure 6 – Simulation of SLJ with three adhesive thickness: a) 0,4 mm, b) 0,8 mm, c) 1,5 mm.

The breaking force (or rupture force) is the maximum load reaches by the simulation, which is considered in the point of damage onset. Thus, after this moment, the displacement still increases, even though the force decrease. Before the damage onset, the maximum stresses occur at the overlap ends (Fig. 7), the place where the adhesive fails. This is agreement with the literature, as seen in the Introduction. After this point, the adhesive layer breaks from the ends towards the center.

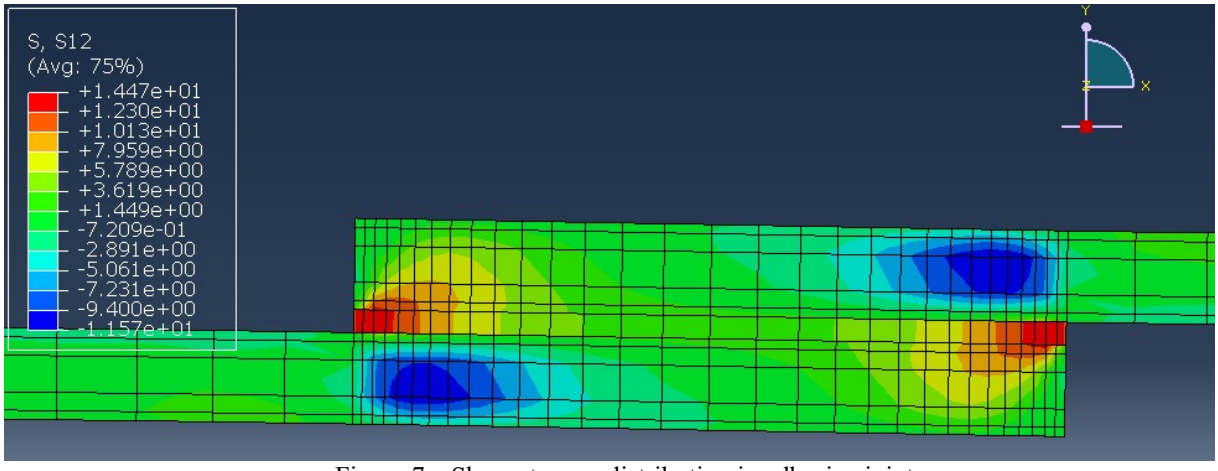


Figure 7 – Shear stresses distribution in adhesive joint.

The difference between the experimental and numerical results are presented in Fig. 8, with the respective standards deviations of the tests. The experimental and numerical results of 0,4 and 0,8 mm adhesive thickness are very similar. For 0,4 mm the difference between each other is less than 100 N, setting a deviation of 2% approximately. For the 0,8 mm thickness, the variation was 79 N, ever lower than the 0,4mm. This result sets a deviation of 2% between the experimental and simulation results. But for the 1,5 mm adhesive thickness the difference between the two results was 1625 N (37 % of deviation). There are some ways to simulate as adhesive joint, which includes different failure models (CZM or von Misses criterion, for example), or yet, different ways to draw the joint. It includes draw a finite thickness (used in this work), or considering zero thickness. Since all of the three simulations used the same mechanical properties, and only the 0,4 and 0,8 mm thickness had good results in comparison with the experimental and numerical results, it suggests that the CZM applied with the methodology used do not leads to accurate results for larger thickness, as the thickness of 1,5 mm.

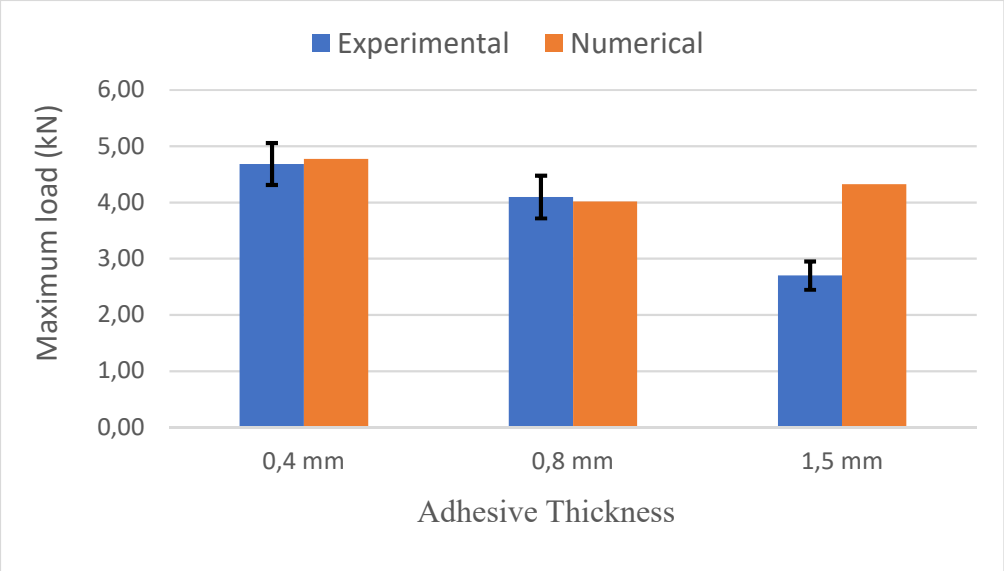


Figure 8 - Comparative graphic between the results obtained from experimental e simulation.

The experimental results are in agreement with several studies stated such as Neto (2017), Naito et al. (2012) and Nascimento (2013), which presented that the rupture force decreases as the adhesive thickness increases. This is what was seen for the three thickness studied (0,4 mm, 0,8 mm and 1,5 mm). As occurred in the work of Neto (2017) for the combined loading joints, the numerical results for the 1,5 mm thickness using the CZM did not present good agreement with the tests for single lap joints. This may have been due to the difficult in DCB test with the ARC 858, that is a brittle adhesive. So, the value of $G_{Ic}$ value may be underestimated, as predict by Neto (2017).

## 4. CONCLUSIONS

The numerical simulation presented good agreement with the experimental analysis. The difference between them were only 2%, except the 1,5 mm adhesive thickness (37%). Moreover, the two lower thicknesses (0,4 and 0,8mm) are in accordance with the literature for experimental results: the lower thickness stands greater forces when compared with larger thickness. The results showed that the larger stresses occur in the overlap ends, as presented in the literature. Theses are the points in the adhesive layer where the failure begins.

There are several options to modelling bonded joints. In this work a continuum approach was used, considering the adhesive as a cohesive element and design it with the real thickness (not zero thickness). The results showed good agreement between numerical and experimental analysis for the 0,4 mm e 0,8 mm thickness. For the 1,5 mm thickness, the results were not satisfactory, just as the work of (Neto, 2017), that also obtained good accordance numerical and experimental for smaller thickness.

This work confirms that CZM with finite thickness do not provide results in accordance with the experiments for 1,5 mm thickness, as occurred in the work of Neto (2017), but for combined loading joints. It may be occurred due to the difficult founded in DCB tests, as stated by Neto (2017), especially due to the brittle adhesive used (ARC 858) in this work, which makes it difficult to follow the crack growth. This work used the same $G_{Ic}$ value obtained by this author, and found similar results, both for small thickness (good results), for both larger thickness (unsatisfactory results).

This work was limited to studying three adhesive thicknesses. Thus, other thicknesses should be investigated, as well as fracture characterization tests, such as DCB and ENF tests. The critical fracture energies should be calculated by different methods from those used by Neto (2017).

## 5. ACKNOWLEDGE

I appreciate the work from UERJ that manufactured all of the specimens here presented and moreover performed some test that was used in this article. Furthermore, I'd like to thank my mentor that helped and guided me along this path.

## 6. REFERENCES

ABAQUS, 2014. Analysis user's guide volume IV: elements, Dassault Systems.

ADAMS, R.D., PEPPIATT, N. A., 1974. *Stress analysis of adhesively-bonded lap joints*. Journal of Strain Analysis.

ADAMS, R. D., COPPENDALE, J., MALLICK, V., AL-HAMDAN, H., 1992. *The effect of temperature on the strength of adhesive joints*. International Journal of Adhesion and Adhesives.

APALAK, M. K., GUNES, R., 2002. *On non-linear thermal stresses in an adhesively bonded single lap joint.* Computers & Structures.

BARNES, T.A., PASHBY, I.R., 1998. *Joining techniques for aluminium spaceframes used in automobiles Part II - adhesive bonding and mechanical fasteners,* International Manufacturing Centre, University of Warwick, Coventry.

CARVALHO, U. T. F., 2016. *Modelação de juntas adesivas por modelos de dano coesivo utilizando o método direto*. Masters dissertation, Instituto Superior de Engenharia do Porto, Porto.

DA SILVA, L. F. M., MAGALHÃES, A. G., MOURA, F. S. F., 2007. *Juntas Adesivas Estruturais.* Publindústria.

DA SILVA, L. F. M., CARBAS, R. J. C., CRITCHLOW, G. W., FIGUEIREDO, M. A. V., BROWN, K., 2009a. *Effect of material, geometry, surface treatment and environment on the shear strength of single lap joints*. International Journal of Adhesion and Adhesives.

DA SILVA, L. F. M., DAS NEVES, P. J. C., ADAMS, R. D., WANG, A., & SPELT, J. K., 2009b. *Analytical models of adhesively bonded joints - Part I: Literature survey*. International Journal of Adhesion and Adhesives.

DA SILVA, A. H. M. F. T., 2010. *Critério de falha para juntas coladas submetidas a carregamentos complexos*. Ph.D. thesis, Universidade Federal Fluminense, Niterói.

FIUZA, G.C.C., 2016. *Análise de comportamento mecânico de juntas coladas multimateriais*, Centro Federal de Educação Tecnológica, Rio de Janeiro.

KAFKALIDIS, M. S., THOULESS, M. D., 2002. *The effects of geometry and material properties on the fracture of single lap-shear joints*. International Journal of Solids and Structures.

KIM, T.H.; KWEON, J.H.; CHOI J, H., 2008. *An experimental study on the effect of overlap length on the failure of composite to aluminum single lap bonded joint*. Journal of Reinforced plastic and composites.

LANG, T. P., MALLICK, P. K., 1998. *Effect of spew geometry on stresses in single lap adhesive joints*, International Journal of Adhesion & Adhesives.

MEDINA, J.A.H, 2014. *Avaliação de previsões de fratura elastoplástica*. Ph.D. thesis. Pontifícia Universidade Católica, Rio de Janeiro.

NASCIMENTO, A. N. S., 2013. *Efeito da espessura do adesivo na resistência de juntas de sobreposição simples na ligação materiais compósitos*. Masters dissertation, Faculdade de Engenharia da Universidade de Porto, Porto.

NETO, R. M. C., 2017. *Análise numérica e experimental de juntas coladas em duas configurações: junta de cisalhamento simples e junta de carregamento combinado*. Masters dissertation. Universidade do Estado do Rio de Janeiro, Friburgo.

NETO, R. M. C., SAMPAIO, E.M., ASSIS, J.T., 2019. *Numerical and experimental analysis of bonded joints with combined loading*. International Journal of Adhesion & Adhesives.

RENTON, W., & VINSON, J., 1975. *The efficient design of adhesive bonded joints*. 16th Structural Dynamics and Materials Conference.

RIBEIRO, M.L., 2009. *Programa para análise de juntas coladas: compósito/compósito e metal/compósito*. Masters dissertation. Universidade de São Paulo, São Carlos.

RIBEIRO, N. F. Q. R., 2012. *Efeito de alterações geométricas na resistência de juntas de sobreposição*. Masters dissertation. Instituto Superior de Engenharia do Porto, Porto.

SHAHID, M., HASHIM, S. A., 2002. *Effect of surface roughness on the strength of cleavage joints*. International Journal of Adhesion and Adhesives.